Composites Part B 101 (2016) 77–86

Contents lists available at ScienceDirect

Composites Part B

journal homepage: www.elsevier.com/locate/compositesb

Friction welding of dissimilar plastic/polymer materials with metal powder reinforcement for engineering applications

Rupinder Singh [a], Ranvijay Kumar [a], Luciano Feo [b], Fernando Fraternali [b, *]

[a] Department of Production Engineering, Guru Nanak Dev Engineering College, Ludhiana, India
[b] Department of Civil Engineering, University of Salerno, Italy

ARTICLE INFO

Article history:
Received 28 May 2016
Accepted 30 June 2016
Available online 4 July 2016

Keywords:
Friction welding
ABS
Nylon6
Shore hardness
Tensile strength
Porosity

ABSTRACT

Friction welding is one of the established processes for joining of similar as well as dissimilar polymer/plastics and metals. In past 20 years numbers of application in different areas using this process have been highlighted, but very limited contributions have been reported on properties of friction welded joints of dissimilar polymer/plastic materials after reinforcement with metal powder. In the present work an attempt has been made to perform friction welding of dissimilar plastic based materials by controlling the melt flow index (MFI) after reinforcement with metal powders. The present studies of friction welding for dissimilar plastic were performed on Lathe by considering three input parameters (namely: rotational speed, feed rate, and time taken to perform welding). Investigations were made to check the influence of process parameters on mechanical and metallurgical properties (like: tensile strength, Shore D hardness and porosity at joint). The process parameters were optimized using Minitab software based on Taguchi L9 orthogonal array and results are supported by photomicrographs.

1. Introduction

The joining of composite materials and structures is a topic of high technological interest; since it is well know that traditional joining techniques are usually not directly exportable to composite elements (refer, e.g. to [1–4] and references therein). Attention is increasingly being given to the following research areas, both experimentally and numerically: fusion bonding [5,6]; welding-based joining techniques [7–14]; friction spot and friction lap joining [15·16],; and ultrasonic joining [17]. Friction welding is a process of joining of materials and structures below their melting points. When these materials come in contact with relative motion to each other, with the action of friction, heat is produced and deformation takes place, due to this intermolecular diffusion is occurred between their faces and thus welding is performed. Friction welding concept was originally come for similar metal joining, but it was further applied for similar thermoplastic composites [18]. Later on this concept was used for the dissimilar materials like steel-aluminum and steel-copper and aluminum-magnesium cylindrical piece joining [19,20] and for dissimilar plastic welding of ABS to HDPE [21]. The number of studies has been reported to check the mechanical, thermal and metallurgical properties of friction welded piece [22–24]. Interface properties are examined to check the fusion, deformation mechanisms and microstructure characteristics of friction welded interface [20,25–26]. ABS and Nylon6 are commonly used thermoplastics with excellent mechanical properties and are used generally for friction welding application [21]. The joining of ABS or Nylon 6 to itself or welding of ABS to HDPE is feasible [27], but, there is a limitation of joint strength (for friction welded joints) of these thermoplastics that hinders its use in different engineering applications.

Some studies have highlighted the use of a tool in the form of a ring which is rotated in between the interface of two pipes. This is getting heated deformed by friction created due to rotation of ring, so welding of pipeline is possible [28]. Friction inertia welding concept is widely accepted in aerospace applications [29,30]. Reinforcement of polymer with nano-composite is the technique to make the feasibility of friction welding process. The studies also highlight that friction spot welding of polymethyl-methacrylate and polymethyl-methacrylate-Sio_2 is feasible [31]. The reinforcement of nano-composite with polymers is responsible for the improved mechanical and metallurgical properties [32–36].

The literature review reveals that joint strength properties of friction welded joints of ABS with Nylon6 are not good enough

* Corresponding author.
E-mail address: f.fraternali@unisa.it (F. Fraternali).

http://dx.doi.org/10.1016/j.compositesb.2016.06.082
1359-8368/

because of difference in their rheological properties (like: melt Flow Index (MFI) and glass transition temperature) [37–41]. But with reinforcement of metal powder in different proportions with these polymers results into similar MFI, which in turns may contribute to better joint strength. So in this study effort has been made to investigate the weld properties of friction welded joints of ABS with Nylon6 after metal powder reinforcement.

2. Experimentation

In pilot experimentation of friction welding for dissimilar plastic/polymer materials, two different materials were judicially selected (namely: ABS and Nylon6). Cylindrical discs of dimension length 50 mm and diameter 25 mm were prepared on hot mounting machine (by pressure moulding). After preparation of cylindrical discs, friction welding was performed on center lathe at 500, 775 and 1200 rpm. Two cylindrical discs were mounted on the center lathe (see Fig. 1), and were put in contact with each other (to generate friction/heat) for duration of 10 s along with automatic feed of 0.045 mm/rev. for 6 s. Welding of these pieces were unsuccessful because ABS and Nylon 6 was not having similar MFI or glass transition temperatures. So, again an experiment was performed with the 10% Fe powder (by weight) as reinforcement of ABS and Nylon6 (without Fe powder reinforcement) work pieces. This time welding was successful. This may be because of attainment of MFI in similar range between two different polymers. Fig. 2 shows friction welded work piece of ABS with 10% Fe powder as reinforcement and Nylon6.

The main objective of this pilot study was to check the possibility of welding for ABS and Nylon6 for engineering applications. For possibility of welding it was necessary to establish MFI of two components in a particular range. So testing was performed on melt flow tester (as per ASTM D 1238 standard) to check the MFI of ABS and Nylon6 with reinforcement of Fe and Al metal powder (see Table 1).

After establishing MFI, for mentioned combination of metal powder with polymers, it was observed that melt flow index of ABS and Nylon 6 are very similar at 40% reinforcement of both metal powder. So, this combination of composition/proportion of metal powder with polymer matrix have been selected for further investigations, with design of experimentation based on Taguchi L9 orthogonal array (see Table 2). Based upon Table 2, Table 3 shows control log of experimentation.

The output parameters for the present study are tensile strength,

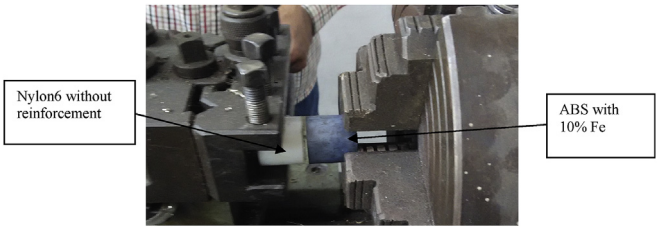

Fig. 1. Pilot experimentation on Center lathe.

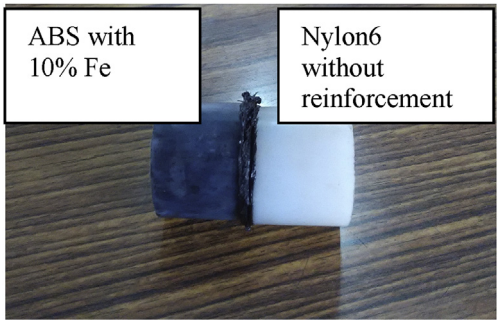

Fig. 2. Obtained welded piece of ABS-10%Fe to Nylon6-10%Fe.

Table 1 MFI of ABS and Nylon6 with reinforcement of Fe and Al metal powder.

MFI with Al powder reinforcement		
Wt% of Al	MFI with ABS	MFI with Nylon 6
0	8.898	9.972
10	9.722	10.622
20	11.114	12.285
30	13.091	13.664
40	14.613	14.656
50	15.250	16.214
MFI with Fe powder reinforcement		
Wt% of Fe	MFI with ABS	MFI with Nylon 6
0	8.898	9.972
10	10.344	11.249
20	11.973	12.615
30	13.681	14.208
40	15.075	15.006
50	16.141	16.786

Table 2
Parameters selected for experimentation Based on Taguchi L9 orthogonal array.

Levels	A Rotational speed (RPM)	B Feed rate(mm/rev)	C Time for welding (s)
1	500	0.045	4
2	775	0.090	6
3	1200	0.180	8

Table 3
Control log of experimentation.

Parametric conditions	A Rotational speed (RPM)	B Feed rate (mm/rev)	C Welding time(s)
1	500	0.045	4
2	500	0.090	6
3	500	0.180	8
4	775	0.045	6
5	775	0.090	8
6	775	0.180	4
7	1200	0.045	8
8	1200	0.090	4
9	1200	0.180	6

Table 4
Shore D hardness value at obtained weld interface (Al metal powder reinforced).

Parametric conditions	Batch run 1	Batch run 2	Batch run 3
1	78.5	78.0	77.5
2	77.5	77.5	78.0
3	77.0	77.5	77.5
4	79.0	78.5	78.0
5	78.0	78.0	77.5
6	77.5	78.0	78.0
7	78.5	78.0	79.0
8	78.0	78.5	78.0
9	78.0	77.5	77.5

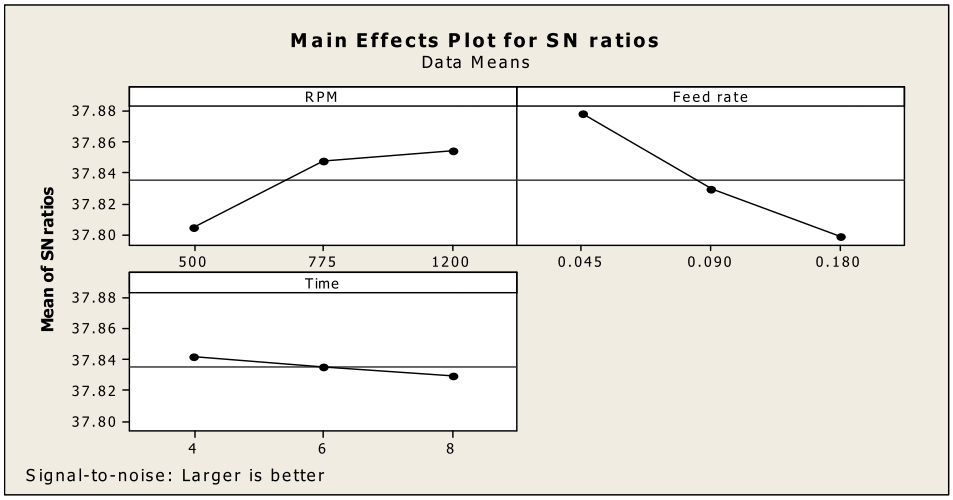

Fig. 3. Main effects plot for SN ratios.

Table 5
Analysis of variance for SN ratios.

Source	Degree of freedom	Sum of square	Adjacent sum of square	Adjacent mean of square	Fisher's value	Probability	Percentage contribution
RPM	2	0.004373	0.004373	0.002186	6.41	0.135	28.95
Feed rate	2	0.009816	0.009816	0.004908	14.40	0.065	64.98
Time	2	0.000236	0.000236	0.000118	0.35	0.743	1.56
Residual Error	2	0.000682	0.000682	0.000341			4.51
Total	8	0.015105					

Table 6
Ranking of input parameters based upon SN ratio for larger the better case.

Level	A(RPM)	B(Feed rate)	C(Welding time)
1	37.80	37.88	37.84
2	37.85	37.83	37.84
3	37.85	37.80	37.83
Delta	0.05	0.08	0.01
Rank	2	1	3

Shore D hardness and porosity at joint. These parameters have been selected to ascertain the functional ability of the welded joints.

3. Result and discussion

After 03 successful batch runs for each combination of metal powder reinforcement as per Taguchi L9 orthogonal array, the results for different output parameters (namely: tensile strength, Shore D hardness and porosity at joint) have been tabulated.

Table 7
Shore D hardness value at obtained weld interface (Fe metal powder reinforced).

Parametric conditions	Batch run 1	Batch run 2	Batch run 3
1	81.5	82.0	82.0
2	81.5	81.5	81.5
3	81.0	80.5	81.0
4	82.5	83.0	81.0
5	82.0	82.0	82.0
6	81.5	81.0	82.0
7	83.0	82.5	83.0
8	82.5	82.0	83.0
9	82.5	82.0	82.5

3.1. Shore D hardness at interface

Shore D hardness test were performed at interface joints of the obtained weld joints (see Table 4).

The above result obtained for Shore D hardness value were further processed for 'larger the better type case' on Minitab Software to check which factor was most responsible for increase in Shore D hardness value at the joint interface. Fig. 3 shows main effect plot for signal to noise (SN) ratio for hardness. As observed from Fig. 3 for maximum hardness 1200 rpm with feed rate 0.045 mm/rev. for 4 s is giving the better results. This may be because at high rpm more heat is generated due to friction, the small quantity of feed may lead to better intermolecular diffusion at joint interface. Further the joining time of 04 s may be justified on the basis of the fact that when for short duration small quantity of feed is provided it may give better diffusion of Fe powder in polymer matrix but when this time is increased the spilling out of metal powder out of polymer matrix may occur which reduces the hardness at the joint.

Tables 5 and 6 shows analysis of variance and ranking of input parameters (based on SN ratio) respectively.

For optimization following formula based upon Taguchi design has been used:

$$\eta_{opt} = m + (m_{A3} - m) + (m_{B1} - m) + (m_{C1} - m)$$

where 'm' is the overall mean of S/N data, m_{A3} is the mean of S/N data for rotational speed at level 3 and m_{B1} is the mean of S/N data for factor feed rate at level 1 and m_{C1} is the mean of S/N data for factor time for welding at level 1.

$y^2_{opt} = (1/10)^{\eta opt/10}$ for properties, lesser is better

$y^2_{opt} = (10)^{\eta opt/10}$ for properties, greater is better

Calculation,
Overall mean of SN ratio (m) was taken from Minitab software.

$m = 37.8350$ db

Now from response table of signal to noise ratio, $m_{A3} = 37.850$, $m_{B1} = 37.880$ and $m_{C1} = 37.840$.

From here, η_{opt}
$= 37.835 + (37.850-37.835) + (37.880-37.835) + (37.840-37.835)$

Now, $y^2_{opt} = (10)^{\eta opt/10}$

$y^2_{opt} = (10)^{37.90/10}$

$y_{opt} = 78.52$

So, Optimum Shore D hardness = 78.32 shore D.

Table 7 shows the hardness values at weld interface with Fe powder reinforcement.

The above result obtained of Shore D hardness value for Fe metal powder reinforcement were further processed for 'larger the better type case' on Minitab Software to check which factor was most responsible for increase in Shore D hardness value at the joint interface. Fig. 4 shows main effect plot for SN ratio for hardness. As observed from Fig. 4 for maximum hardness 1200 rpm with feed rate 0.045 mm/rev. for 8 s is giving the better results. This may be because at high rpm more heat is generated due to friction, the small quantity of feed may lead to better intermolecular diffusion at joint interface.

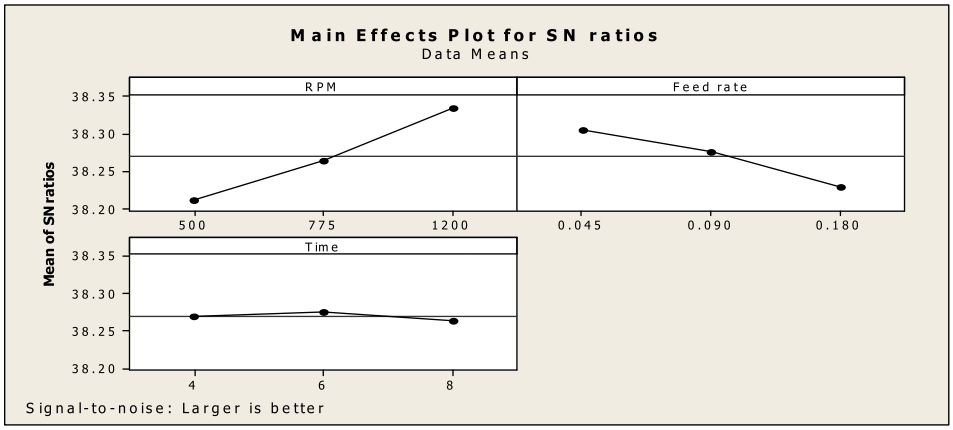

Fig. 4. Main effects plot for SN ratios.

Table 8
Analysis of variance for SN ratios.

Source	Degree of freedom	Sum of square	Adjacent sum of square	Adjacent mean of square	Fisher's value	Probability	Percentage contribution
A	2	0.023081	0.023081	0.011541	25.84	0.037	69.73
B	2	0.008916	0.008916	0.004458	9.98	0.091	26.93
C	2	0.000205	0.000205	0.000103	0.23	0.813	0.61
Residual Error	2	0.000893	0.000893	0.000447			2.69
Total	8	0.033096					

Table 9
Ranking of input parameters based upon SN ratio for larger the better case.

Level	A(RPM)	B(Feed rate)	C(Welding time)
1	38.21	38.31	38.27
2	38.26	38.28	38.28
3	38.33	38.23	38.26
Delta	0.12	0.08	0.01
Rank	1	2	3

$\eta_{opt} = 37.90$ db

Table 10
Tensile strength (kg/mm^2) of welded joint (Al powder reinforced).

Parametric conditions	Batch run 1	Batch run 2	Batch run 3
1	0.4582	0.4056	0.4875
2	0.3625	0.2864	0.4231
3	0.2301	0.2684	0.2015
4	0.4974	0.4056	0.5628
5	0.3521	0.4623	0.2865
6	0.2531	0.2845	0.228
7	0.5375	0.4756	0.5268
8	0.3120	0.3587	0.2821
9	0.4051	0.4265	0.3845

Tables 8 and 9 shows analysis of variance and ranking of input parameters (based on SN ratio) respectively.

The optimum value for Shore D hardness value is calculated = 82.92 shore D.

3.2. Tensile strength of obtained weld piece

Table 10 shows tensile strength of welded joints with Al powder reinforcement.

The above result obtained of tensile strength, were further processed for 'larger the better type case' on Minitab Software to check which factor was most responsible for increase in tensile strength at the joint interface. Fig. 5 shows main effect plot for SN ratio for tensile strength. As observed from Fig. 5 for maximum

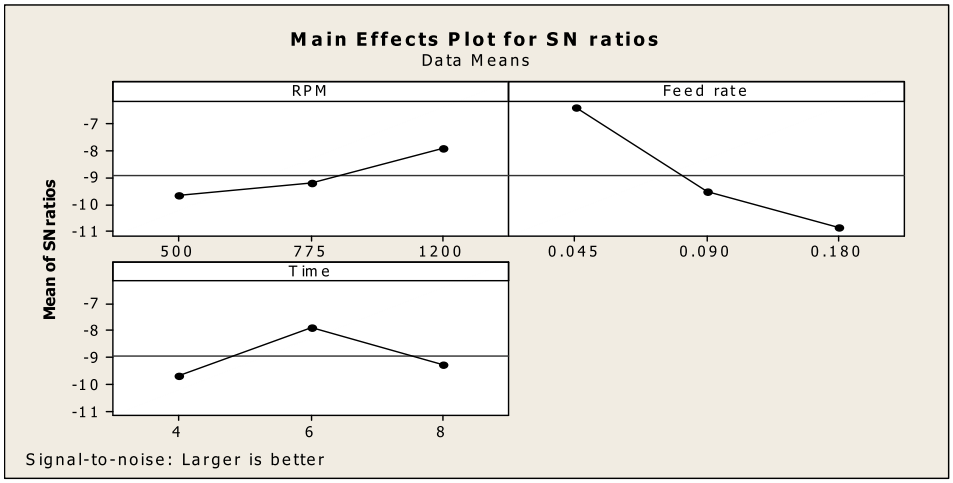

Fig. 5. Main effects plot for SN ratios.

Table 11
Analysis of variance for SN ratios.

Source	Degree of freedom	Sum of square	Adjacent sum of square	Adjacent mean of square	Fisher's value	Probability	Percentage contribution
A	2	5.008	5.008	2.504	1.06	0.485	10.80
B	2	31.171	31.171	15.585	6.62	0.131	67.26
C	2	5.454	5.454	2.727	1.16	0.463	11.76
Residual Error	2	4.607	4.707	2.353			9.94
Total	8	46.339					

Table 12
Ranking of input parameters based upon SN ratio for larger the better case.

Level	A(RPM)	B(Feed rate)	C(Welding time)
1	−9.699	−6.431	−9.682
2	−9.203	−9.519	−7.867
3	−7.928	−10.880	−9.281
Delta	1.771	4.448	1.815
Rank	3	1	2

Table 13
Tensile strength (kg/mm^2) of welded joint (Fe metal powder reinforced).

Parametric conditions	Batch run 1	Batch run 2	Batch run 3
1	0.2209	0.2144	0.2351
2	0.1920	0.2014	0.1898
3	0.1494	0.1568	0.1601
4	0.2367	0.2412	0.2405
5	0.1564	0.1432	0.1398
6	0.1265	0.1354	0.1324
7	0.2204	0.2304	0.2247
8	0.1489	0.1542	0.1486
9	0.1344	0.1236	0.1458

tensile strength 1200 rpm with feed rate 0.045 mm/rev. for 8 s is giving the better results. This may be because at high rpm and low feed rate there was a proper heat generated for intermolecular diffusion. Further joining time 08 s is responsible for the regular diffusion of metal powder with polymers which was responsible for the better joining properties.

Tables 11 and 12 shows analysis of variance and ranking of input parameters (based on SN ratio) respectively.

The optimum tensile strength for Al powder reinforced sample is calculated = 0.6067 kg/mm^2

Table 13 shows tensile strength of welded joints with Fe powder reinforcement.

The above result obtained of tensile strength, were further processed for 'larger the better type case' on Minitab Software to check which factor was most responsible for increase in tensile strength at the joint interface. Fig. 6 shows main effect plot for SN ratio for tensile strength. As observed from Fig. 6 for maximum tensile strength 775 rpm with feed rate 0.045 mm/rev. for 6 s is giving the better results. This may be because at medium rpm condition optimum heat generated due to friction, the small quantity of feed may lead to better intermolecular diffusion at joint interface. Further joining time 06 s is responsible for the regular diffusion of metal powder with polymers which was responsible for the better joining properties.

Tables 14 and 15 shows analysis of variance and ranking of input parameters (based on SN ratio) respectively.

The optimum tensile strength for Fe powder reinforced sample = 0.2657 kg/mm^2.

3.3. Porosity percentage (%age) at joint interface

Table 16 shows porosity %age at joint interface with Al powder reinforcement. Based upon Table 16, Fig. 7 shows mean effect plot for SN ratio for smaller is better type case (as one is interested in less porosity). As observed from Fig. 7 the best settings for controlling the porosity are 500 rpm, 0.090 mm/rev feed and joining time of 4sec.

Tables 17 and 18 shows analysis of variance and ranking of input parameters (based on SN ratio) respectively.

The optimum porosity for Al powder reinforced sample = 6.8622%.

Table 19 shows porosity %age at joint interface with Fe powder reinforcement. Based upon Table 19, Fig. 8 shows mean effect plot for SN ratio for smaller is better type case (as one is interested in less porosity). As observed from Fig. 8 the best settings for controlling the porosity are 775 rpm, 0.044 mm/rev feed and joining

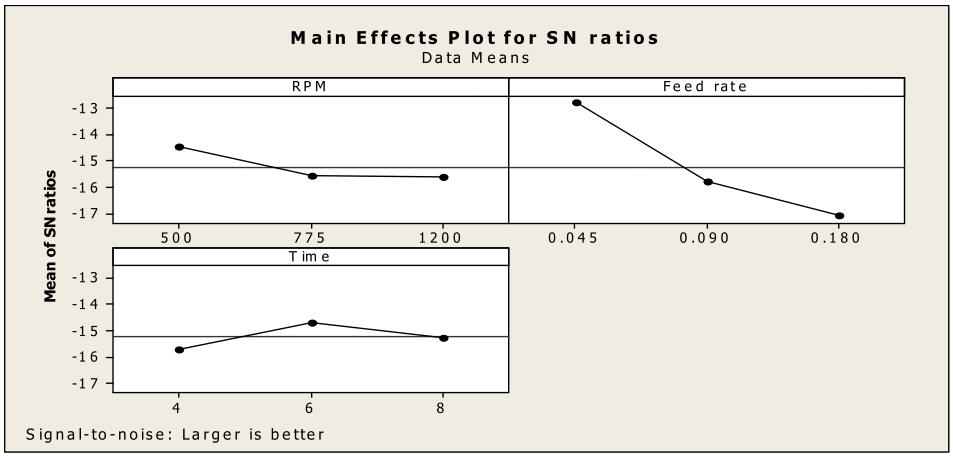

Fig. 6. Main effects plot for SN ratios.

Table 14
Analysis of variance for SN ratios.

Source	Degree of freedom	Sum of square	Adjacent sum of square	Adjacent mean of square	Fisher's value	Probability	Percentage contribution
A	2	2.533	2.533	1.2667	2.15	0.317	7.37
B	2	29.135	29.135	14.5673	24.76	0.039	84.82
C	2	1.503	1.503	0.7514	1.28	0.439	4.37
Residual Error	2	1.177	1.177	0.5883			3.42
Total	8	34.347					

Table 15
Ranking of input parameters based upon SN ratio for larger the better case.

Level	A(RPM)	B(Feed rate)	C(Welding time)
1	−14.48	−12.80	−15.71
2	−15.59	−15.80	−14.71
3	−15.63	−17.10	−15.28
Delta	1.14	4.30	1.00
Rank	2	1	3

Table 16
Porosity %age at obtained weld joint (Al powder reinforced).

Parametric conditions	Batch run 1	Batch run 2	Batch run 3
1	8.78	11.24	7.54
2	7.28	14.54	6.63
3	17.47	17.27	12.34
4	16.80	15.58	14.87
5	15.71	15.35	17.54
6	14.15	14.51	13.54
7	19.56	17.54	18.75
8	7.16	7.88	6.87
9	17.84	18.56	16.84

time of 8sec.

Tables 20 and 21 shows analysis of variance and ranking of input parameters (based on SN ratio) respectively. The optimum porosity for Fe powder reinforced sample = 24.154%. The results of different mechanical properties are in line with the observations made by other investigators [38–43].

3.4. Optical micrograph observations at joint

Fig. 9 shows the micrographic observations of welding joint at magnification of 100× at different parametric conditions based on Taguchi L9 orthogonal array. The behavior and characteristics of micrograph at joint is responsible for the mechanical and metallurgical properties variations. Regarding the Shore D hardness, the maximum value 7.0 Shore D was obtained at parametric condition 4 means combination of 775 RPM, 0.045 mm/rev and 6 s welding time. If we see the micrograph at parametric conditions 4, there is a large accumulation of aluminum powder at joint interface occurred due to low feed rate, which is responsible for the greater hardness

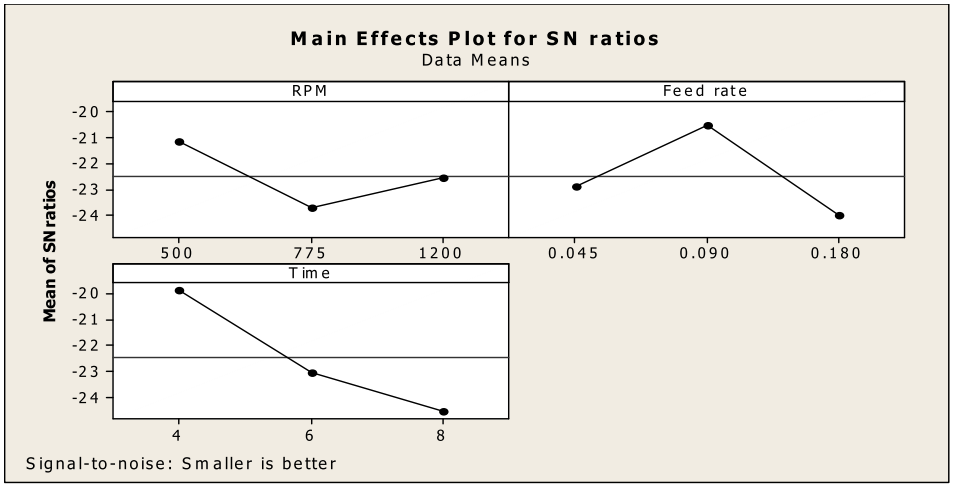

Fig. 7. Main effects plot for SN ratios.

Table 17
Analysis of variance for SN ratios.

Source	Degree of freedom	Sum of square	Adjacent sum of square	Adjacent mean of square	Fisher's value	Probability	Percentage contribution
A	2	9.692	9.692	4.846	4.05	0.198	14.96
B	2	18.736	18.736	9.368	7.83	0.113	28.93
C	2	33.933	33.933	16.967	14.17	0.066	52.40
Residual Error	2	2.394	2.394	1.197			3.69
Total	8	64.755					

Table 18
Ranking of input parameters based upon SN ratio for Smaller is better.

Level	A(RPM)	B(Feed rate)	C(Welding time)
1	−21.17	−22.92	−19.88
2	−23.71	−20.54	−23.02
3	−22.56	−23.99	−24.54
Delta	2.54	3.45	4.66
Rank	3	2	1

Table 19
Porosity %age at obtained weld joint (Fe powder reinforced).

Parametric conditions	Batch run 1	Batch run 2	Batch run 3
1	26.26	25.96	26.84
2	27.22	29.10	28.45
3	28.63	27.56	28.56
4	23.45	25.65	23.56
5	28.80	25.88	28.56
6	27.25	25.66	26.78
7	23.03	26.54	25.65
8	24.68	28.45	26.45
9	28.70	25.64	31.25

at joint. Similarly, minimum value obtained for parametric conditions 3 which is the combination of 500 RPM, 0.180 mm/rev and welding time of 8 s, shows in micrograph that there was a dispersion of metallic powder with plastic material occurred due to high feed rate that caused the lower hardness value at joint interface. Observations were made regarding the tensile strength, maximum value obtained at parametric conditions 7, combination of 1200 RPM, 0.045 mm/rev and welding time of 8 s shows that there was a strong diffusion occurred between the metal powder and plastic due to high speed and low feed conditions, which was responsible for the better tensile properties. Similarly, minimum value was obtained at parametric condition 3 which was the combination of 500 RPM, 0.180 and welding time for 6 s; due to low speed and high feed rate conditions there was dispersion of metal powder occurred that caused the poor tensile strength. Observations were taken regarding the percentage porosity at joint shows that best porosity obtained 7.16% at parametric condition 8 which was the combination of 1200 RPM, 0.090 mm/rev and welding time of 4 s. Due to high speed and low welding time, metal powder accumulates at joint with less void fashion that was responsible for the less porosity at joint. Similarly, poor porosity obtained 19.56% at parametric combination of 1200 RPM, 0.045 mm/rev and welding time of 8 s, due to higher welding time there was a random mixing of metal powder and plastic material occurred that was responsible

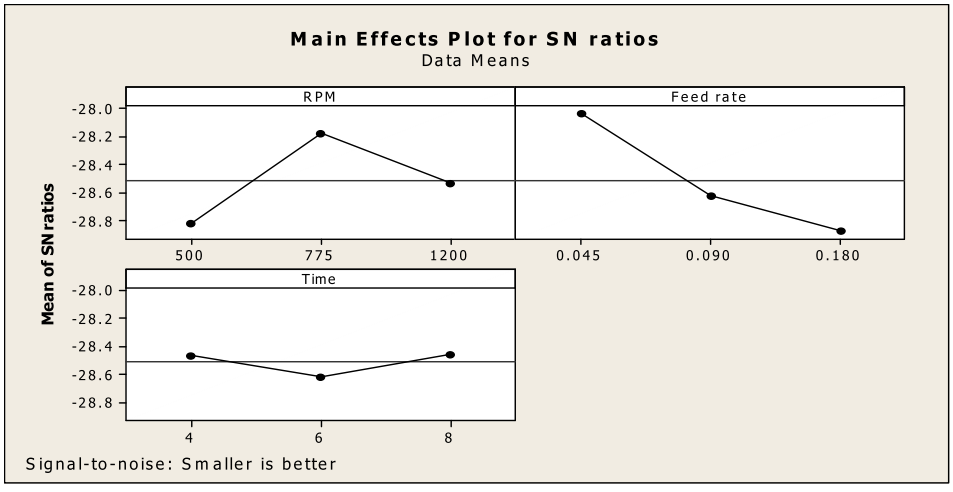

Fig. 8. Main effects plot for SN ratios.

Table 20
Analysis of variance for SN ratios.

Source	Degree of freedom	Sum of square	Adjacent sum of square	Adjacent mean of square	Fisher's value	Probability	Percentage contribution
A	2	0.62418	0.62418	0.31209	7.48	0.118	33.17
B	2	1.12588	1.12588	0.56294	13.50	0.069	59.83
C	2	0.04818	0.04818	0.02409	0.58	0.634	2.56
Residual Error	2	0.08342	0.08342	0.04171			4.43
Total	8	1.88166					

Table 21
Ranking of input parameters based upon SN ratio for Smaller is better.

Level	A(RPM)	B(Feed rate)	C(Welding time)
1	−28.82	−28.04	−28.46
2	−28.18	−28.62	−28.62
3	−28.54	−28.88	−28.46
Delta	0.64	0.85	0.16
Rank	2	1	3

for poor porosity at joint.

Fig. 10 shown the micrographic observations at welded joint with Fe powder reinforcement, as similar to Al powder reinforcement the observations were made at 100× magnification. Regarding Shore D hardness value, the maximum value was 83.0 Shore D obtained at parametric condition 7 was the combination of 1200 RPM, 0.045 mm/rev and for welding tome of 8 s. There an accumulation of metal powder occurred at joint due to high speed and low feed rate caused the better shore D hardness. Similarly, minimum value 81.0 obtained at parametric condition of 500 RPM, 0.180 mm/rev and for welding time of 8 s, there was a lack of metallic powder phase at interface due to low speed and high feed and time, which caused the poor value of Shore D hardness. Regarding tensile properties of Fe powder reinforced welded joints; observations shows that due to less accumulation of metal power at interface a less effective bonding occurred that caused the lower in tensile strength as compared to the aluminum metal powder reinforced samples. The best tensile value 0.2367 kg/mm^2 was obtained at parametric condition 4, combination of 775 RPM, 0.045 mm/rev and welding time of 6 s. Again due to low feed rate the metal powder accumulated and hence it caused the better tensile properties.

The minimum tensile strength 0.1265 kg/mm^2 was obtained at parametric condition 6, combination of 775RPM, 0.180 mm/rev

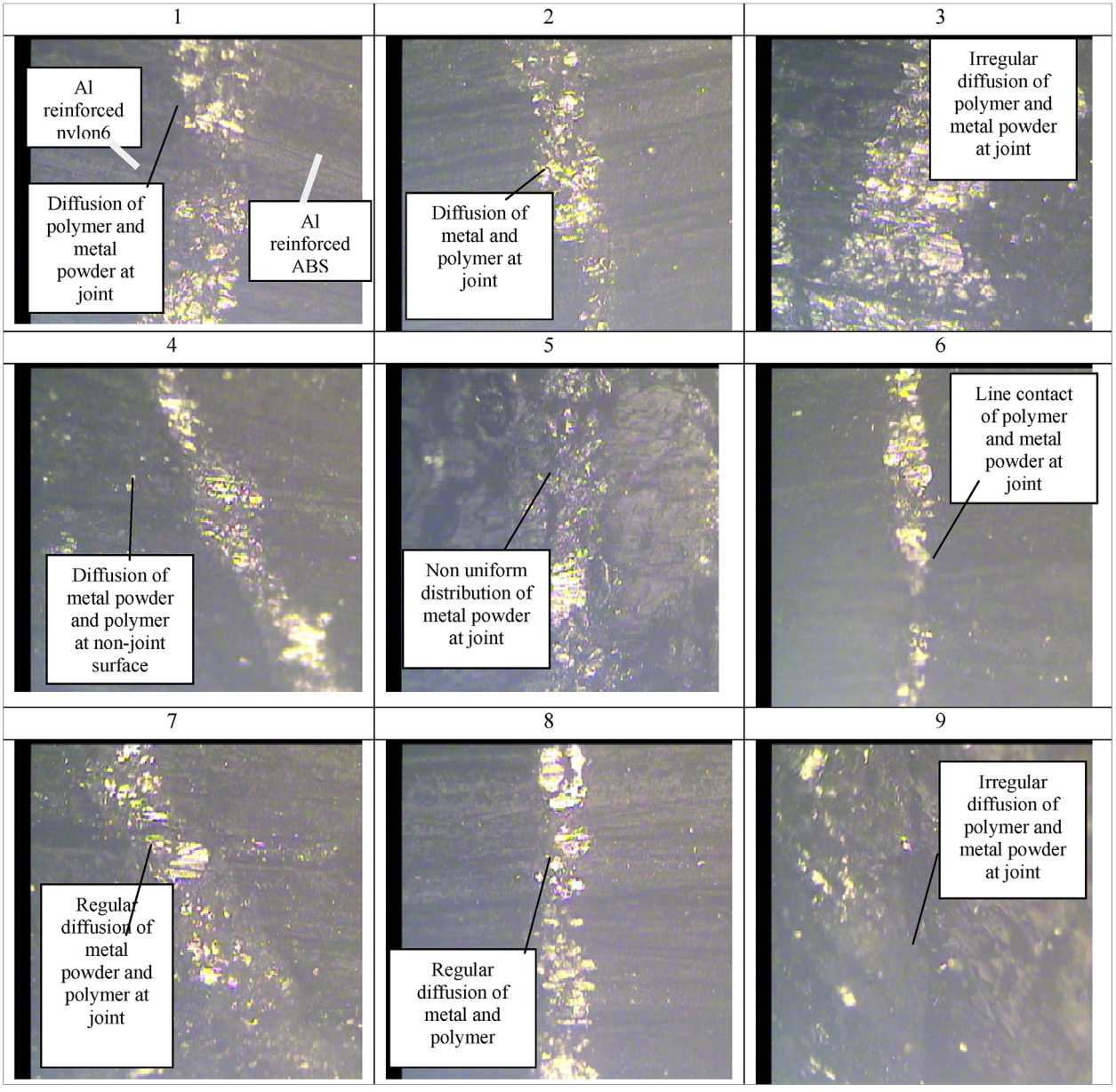

Fig. 9. Optical micrographic View for Al powder reinforced joints at 100× magnification.

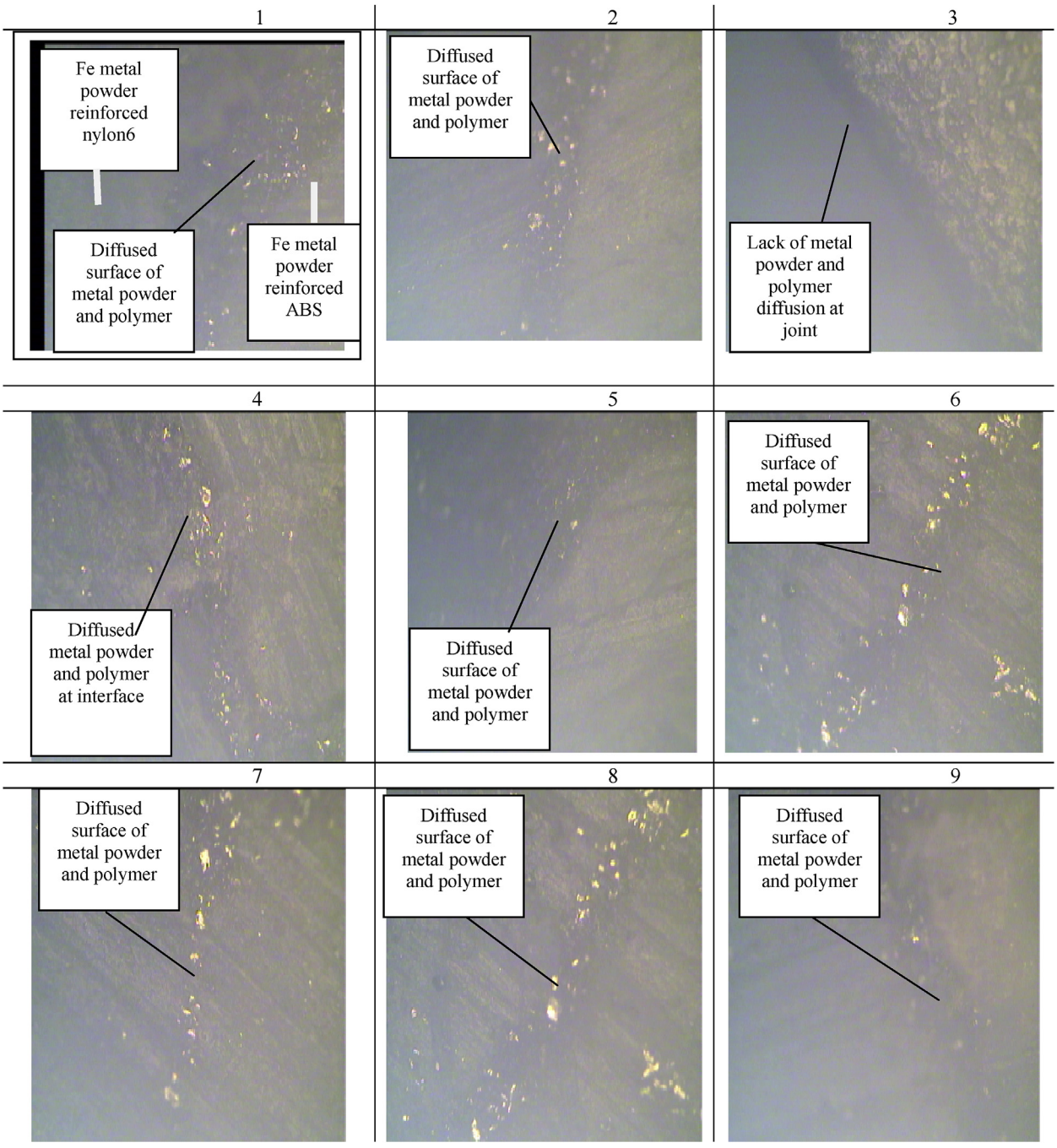

Fig. 10. Optical micrographic view for Fe powder reinforced joints at 100× magnification.

and for welding time of 4 s. There was irregular formation of metal powder was occurred at interface due to high feed rate caused the lower value of tensile strength. Further investigations were made regarding porosity percentage at joint interface shown that the porosity was as poorer, as compared to the aluminum metal powder reinforcement. The best value for porosity was 23.03% obtained at parametric condition of 7 combinations of 1200RPM, 0.045 mm/rev and welding time of 8 s. Due to high speed there line formation of metal powder was occurred at joint, which results into the better control of porosity. The maximum value of porosity 28.80% was obtained at parametric condition 5; combinations of 775RPM, 0.045 mm/rev and for 8 s welding time. Due to higher welding time, metal powders were dispersed and void formation taken place responsible for the poor value of porosity at joint.

4. Conclusions

This study highlights the best settings of input parameters of friction welding process for joining of dissimilar polymer/plastic materials with metal powder reinforcement. Two separate case studies one of Al powder reinforcement and second of Fe powder reinforcement has been outlined. The results of study suggests that dissimilar polymer materials with metal powder reinforcement can be joined together successfully by using the proposed methodology. Following are the conclusions of the present study.

For welding of Al metal powder reinforcement

- The parameter obtained for friction welding of best Shore D hardness value i.e. 79.0, was found at parameter combination of 775 RPM, 0.045 rev/mm and 6 s of welding time.
- The parameter obtained for friction welding of Tensile strength i.e. 0.5375 kg/sq mm, was found at parameter combination of 1200 RPM, 0.045 rev/mm and 8 s of welding time.
- The parameter obtained for friction welding of %age porosity i.e. 7.16%, was found at parameter combination of 1200 RPM, 0.090 rev/mm and 4 s of welding time.

For welding of Fe metal powder reinforcement

- The parameter obtained for friction welding of best Shore D hardness value i.e. 83.0, was found at parameter combination of 1200 RPM, 0.045 rev/mm and 8 s of welding time.
- The parameter obtained for friction welding of Tensile strength i.e. 0.2367 kg/sq mm, was found at parameter combination of 775 RPM, 0.045 rev/mm and 6 s of welding time
- The parameter obtained for friction welding of %age porosity i.e. 23.03%, was found at parameter combination of 1200 RPM 0.045, rev/mm and 8 s of welding time.

Acknowledgement

The authors would like to thank Manufacturing Research Lab (Production Engineering, GNDEC Ludhiana) and Institution of Engineers (India), Grant Number: PG2016011 for financial support for this project.

References

[1] Ageorges C, Ye L, Hou M. Advances in fusion bonding techniques for joining thermoplastic matrix composites: a review. Compos Part A Appl S 2001;32(6):839–57.
[2] Deng S, Djukic L, Paton R, Ye L. Thermoplastic-epoxy interactions and their potential applications in joining composite structures - a review. Compos Part A Appl S 2015;68:121–32.
[3] Heshmati M, Haghani R, Al-Emrani M. Environmental durability of adhesively bonded FRP/steel joints in civil engineering applications: state of the art. Compos Part B Eng 2015;81:259–75.
[4] Korta J, Mlyniec A, Uhl T. Experimental and numerical study on the effect of humidity-temperature cycling on structural multi-material adhesive joints. Compos Part B Eng 2015;79:621–30.
[5] Xie L, Liu H, Wu W, Abliz D, Duan Y, Li D. Fusion bonding of thermosets composite structures with thermoplastic binder co-cure and prepreg interlayer in electrical resistance welding. Mater Des 2016;98:143–9.
[6] Fan H, Vassilopoulos AP, Keller T. Experimental and numerical investigation of tensile behavior of non-laminated CFRP straps. Compos Part B Eng 2016;91:327–36.
[7] Cioffi F, Fernández R, Gesto D, Rey P, Verdera D, González-Doncel G. Friction stir welding of thick plates of aluminum alloy matrix composite with a high volume fraction of ceramic reinforcement. Compos Part A Appl S 2013;54:117–23.
[8] Villegas IF. Strength development versus process data in ultrasonic welding of thermoplastic composites with flat energy directors and its application to the definition of optimum processing parameters. Compos Part A Appl S 2014;65:27–37.
[9] Shi H, Villegas IF, Octeau M-A, Bersee HEN, Yousefpour A. Continuous resistance welding of thermoplastic composites: modelling of heat generation and heat transfer. Compos Part A Appl S 2015;70:16–26.
[10] Fernandez Villegas I, Vizcaino Rubio P. On avoiding thermal degradation during welding of high-performance thermoplastic composites to thermoset composites. Compos Part A Appl S 2015;77:172–80.
[11] Braga DFO, De Sousa LMC, Infante V, Da Silva LFM, Moreira PMGP. Aluminium friction-stir weld-bonded joints. Adhesion 2016;92(7–9):665–78.
[12] Kumar S. Ultrasonic assisted friction stir processing of 6063 aluminum alloy. Arch Civ Mech Eng 2016;16(3):473–84.
[13] Mishra RR, Sharma AK. Microwave-material interaction phenomena: heating mechanisms, challenges and opportunities in material processing. Compos Part A Appl S 2016;81:78–97.
[14] Goushegir SM, Dos Santos JF, Amancio-Filho ST. Failure and fracture micromechanisms in metal-composite single lap joints produced by welding-based joining techniques. Compos Part A Appl S 2016;81:121–8.
[15] André NM, Goushegir SM, Dos Santos JF, Canto LB, Amancio-Filho ST. Friction Spot Joining of aluminum alloy 2024-T3 and carbon-fiber-reinforced poly(-phenylene sulfide) laminate with additional PPS film interlayer: microstructure, mechanical strength and failure mechanisms. Compos Part B Eng 2016;94:197–208.
[16] Nagatsuka K, Yoshida S, Tsuchiya A, Nakata K. Direct joining of carbon-fiber-reinforced plastic to an aluminum alloy using friction lap joining. Compos Part B Eng 2015;73:82–8.
[17] Feistauer EE, Guimarães RPM, Ebel T, Dos Santos JF, Amancio-Filho ST. Ultrasonic joining: a novel direct-assembly technique for metal-composite hybrid structures. Mater Lett 2016;170:1–4.
[18] Taylor NS, Jones SB, Weld M. The feasibility of welding thermoplastic composite materials. Constr Build Mater 1989;3(4):213–9.
[19] Yilbas BS, Şahin AZ, Kahramanb N, Al-Garni AZ. Friction welding of StAl and AlCu materials. J Mater Process Technol 1995;49(3–4):431–43.
[20] Kostka A, Coelho RS, Santos JD, Pyzalla AR. Microstructure of friction stir welding of aluminium alloy to magnesium alloy. Scr Mater 2009;60(11):953–6.
[21] Gao J, Li C, Shilpakar U, Shen Y. Improvements of mechanical properties in dissimilar joints of HDPE and ABS via carbon nanotubes during friction stir welding process. Mater Des 2015;86:289–96.
[22] Sluzalec A. Thermal effects in friction welding. Int J Mech Sci 1990;32(6):467–78.
[23] Stokes VK, Hobbs SY. Vibration welding of ABS to itself and to polycarbonate, poly(butylene terephthalate), poly(ether imide) and modified poly(phenylene oxide). J Polym 1993;34(6):1222–31.
[24] Stokes VK. The effect of fillers on the vibration welding of poly(butylene Terephthalate). J Polym 1993;34(21):4445–54.
[25] Yılmaz M, Col M, Acet M. Interface properties of aluminum/steel friction welded components. Mater Charact 2002;49(5):421–9.
[26] Rotundo F, Ceschini L, Morri A, Jun TS, Korsunsky AM. Mechanical and microstructural characterization of 2124Al/25 vol.%SiCp joints obtained by linear friction welding (LFW). Compos Part A Appl S 2010;41(9):1028–37.
[27] Panneerselvam K, Lenin K. Joining of Nylon 6 plate by friction stir welding process using threaded pin profile. Mater Des 2014;53:302–7.
[28] Faes K, Dhooge A, Baets PD, Donckt EV, Waele WD. Parameter optimisation for automatic pipeline girth welding using a new friction welding method. Mater Des 2009;30(3):581–9.
[29] Attallah MM. Inertia friction welding (IFW) for aerospace applications. In: Chaturvedi M, editor. Welding and joining of aerospace materials. Woodhead Publishing; 2012. p. 25–74.
[30] Raab U, Levina S, Wagnera L, Heinze C. Orbital friction welding as an alternative process for blisk manufacturing. J Mater Process Technol 2015;215(1):189–92.
[31] Junior WS, Handge UA, Jorge F, Abetz V, Filho STA. Feasibility study of friction spot welding of dissimilar singlelap joint between poly(methyl methacrylate) and poly(methyl methacrylate)SiO2 nanocomposite. Mater Des 2014;215:246–50.
[32] D'Alvise L, Massoni E, Walloe SJ. Finite element modelling of the inertia friction welding process between dissimilar materials. J Mater Process Technol 2002;125–126(9):387–91.
[33] Healy JJ, McMullan DJ, Bahrani AS. Analysis of frictional phenomena in friction welding of mild steel. Wear 1976;37(2):265–78.
[34] Hoseinlaghab S, Seyed MS, Sadeghian N, Jalili I, Azarbarmas M, Givi MKB. Influences of welding parameters on the quality and creep properties of friction stir welded polyethylene plates. Mater Design.
[35] Inaniwa S, Kurabe Y, Miyashita Y, Hori H. Application of friction stir welding for several plastic materials. In: Proceedings of the 1st international joint symposium on joining and welding Osaka 2013, Japan; 2013. p. 137–42.
[36] Ji Y, Chai Z, Zhao D, Wu S. Linear friction welding of Ti–5Al–2Sn–2Zr–4Mo–4Cr alloy with dissimilar microstructure. J Mater Process Technol 2014;214(4):979–87.
[37] Kolbasuk GM. Hot wedge fusion welding of HDPE geomembranes. Geotext Geomembr 1990;9(4–6):305–17.
[38] Kumar N, Yuan W, Mishra RS. Friction stir welding of dissimilar alloys and materials, chap. 2. Oxford, UK: Butterworth-Heinemann; 2015.
[39] Mercana S, Aydin S, Ozdemir N. Effect of welding parameters on the fatigue properties of dissimilar AISI 2205–AISI 1020 joined by friction welding. Int J Fatigue 2015;81:78–90.
[40] Su JQ, Nelson TW, Sterling CJ. Friction stir processing of large area bulk UFG aluminum alloys. Scr Mater 2005;52(2):135–40.
[41] Singh R, Singh S, Fraternali F. Development of in-house composite wire based feed stock filaments of fused deposition modelling for wear-resistant materials and structures. Compos Part B Eng 2016;98:244–9.
[42] Winiczenko R, Kaczorowski M. Friction welding of ductile iron with stainless steel. J Mater Process Technol 2013;213(3):453–62.
[43] Zimmerman J, Wlosinski W, Lindemann ZR. Thermomechanical and diffusion modelling in the process of ceramic–metal friction welding. J Mater Process Technol 2009;209(4):1644–53.